THE IRAQI JOURNAL OF
VETERINARY MEDICINE
eISSN:2410-7409
pISSN: 1609-5693

OPEN ACCESS

Preparation and Characterization of Bovine Small Intestine Submucosa (SIS) Hydrogel

Saddam K Hummadi*[1], Nadia HR Al-Falahi[2]

[1]Department of Surgery and Obstetrics, Faculty of Veterinary Medicine, Tikrit University, Tikrit, Iraq,
[2]Department of Veterinary Surgery and Obstetrics, College of Veterinary Medicine, University of Baghdad, Baghdad, Iraq

***Correspondence**:
surgeon@tu.edu.iq
Received: 06 June 2023
Revised: 25 June 2023
Accepted: 07 August 2023
Published: 28 December 2023

DOI:
https://doi.org/10.30539/ijvm.v47i2.1479

Cite:
Hummadi SK, Al-Falahi NHR. Preparation and Characterization of Bovine Small Intestine Submucosa (SIS) Hydrogel. Iraqi J. Vet. Med. 2023;47(2):15-22.

A B S T R A C T

The aim of this study was to prepare and characterize a small intestine submucosa (SIS) hydrogel as a bio-scaffold. In this study, SIS from five calves, aged 8-12 months and weighing 250-300 kg, was obtained from a slaughterhouse immediately after slaughtering. The SIS was then decellularized, powdered, and subsequently transformed into a hydrogel. This transformation was achieved by dissolving the decellularized SIS powder in phosphate-buffered saline (PBS) at a concentration of 50% w/v, and allowing it to form a hydrogel over a 12-hour period at 37 °C. Characterization of the SIS hydrogel was conducted using various techniques. Fourier Transform Infrared Spectroscopy (FTIR) was employed to identify the chemical structure of the hydrogel, revealing three primary peaks at 1639 cm^{-1}, 1571 cm^{-1}, and 1338 cm^{-1}, corresponding to amide I, II, and III bands, respectively. Additionally, a broad signal at 3440 cm^{-1} was observed, indicative of the hydroxyproline side chain. The hydrogel's swelling capacity was evaluated, showing an expansion of 437% after a 12-hour immersion in PBS at a pH of 7.4. Scanning Electron Microscopy (SEM) analysis of the lyophilized hydrogel revealed a highly porous and interconnected architecture, resembling a honeycomb structure. Moreover, the hydrogel's antibacterial efficacy was assessed against *Staphylococcus aureus* using an agar diffusion test, which demonstrated a zone of inhibition measuring 16.11 mm. The combined chemical, morphological, and antibacterial properties of the SIS hydrogel developed in this study suggest its potential as a promising bio-scaffold for inducing tissue regeneration and restoring tissue function.

Keywords: small intestine submucosa, decellularization, hydrogel, extracellular matrix

INTRODUCTION

The field of tissue engineering encompasses a diverse array of methods aimed at creating biological substitutes for the regeneration of diseased or damaged tissues (1, 2). A crucial aspect of this field is the development of bio-scaffolds. These are three-dimensional structures designed to mimic the natural extracellular matrix (ECM), facilitating cell adhesion, proliferation, and differentiation (3-6).

Various decellularized tissues have gained prominence as natural biomaterials, offering an alternative to synthetic options for tissue regeneration. These include small intestine submucosa (SIS), liver, heart, kidney, and skin, among others (7, 8). Compared to synthetic biomaterials, natural biomaterials demonstrate several advantages in terms of biodegradability, biological properties, and biocompatibility, closely resembling the native ECM (9-11).

Decellularization is a process that removes intracellular components from tissues while preserving the original ECM

structure. This process involves a combination of physical, chemical, and enzymatic methods (12). SIS has been clinically evaluated for the reconstruction of different organs, including the urethra, lung, and vagina (13). Composed of a range of biomolecules such as collagen, integrin proteins, and four types of glycosaminoglycans (heparin sulphate, chondroitin sulphate, keratin sulphate, and hyaluronan), SIS plays a pivotal role in promoting cell attachment and proliferation, thereby accelerating tissue repair and regeneration (13, 14). A significant advantage of SIS is its derivation from xenogeneic animal species, broadening its applicability in tissue engineering (15).

A hydrogel is a three-dimensional structure composed of highly hydrated polymeric substances that can absorb a lot of water and hold it there while maintaining their structural integrity according to physical and chemical crosslinks (16). Hydrogel derived from SIS have played an important role in regulating various cellular functions better than native SIS. That goes back to the hydrogel supply three-dimensional structural support for cells, as they offer a highly hydrated, cytocompatibility environment, and ease the transfer of nutrients and waste (17).

The SIS hydrogel formed from a collagen-based self-assembly process with presence of proteoglycans, ECM proteins, and glycosaminoglycans. Consequently, the proteins that persist after decellularization and the native biochemical profile of the source tissue will have an impact on polymerization kinetics (9). Hydrogels derived from natural tissues after decellularized retain the structural characteristics and stimulatory properties which can enhance the attachment, growth, migration, and proliferation of cells (18). The present study discusses the preparation of hydrogel from decellularized small intestinal submucosa with defined physical, chemical, and antibacterial features to determine whether the prepared hydrogel can practically be used as a bio-scaffold serving as a biological substitute for the treatment of wounds (In press article.

MATERIALS AND METHODS

Ethical Approval

All procedures used in this study received Ethical approval, which was granted through the local committee of animal care and use at the College of Veterinary Medicine within the University of Baghdad (Number 915 at 24/4/2022) before starting this study.

Preparation of Decellularized SIS Membrane

The process for preparing and evaluating decellularized SIS membrane is depicted in Figure 1 A-F. Five calves, aged between 8-12 months and weighing approximately 250-300 kg, were used for obtaining small intestines from a local slaughterhouse immediately post-slaughter. The serosal surface was thoroughly cleaned to remove connective and adipose tissues, along with any residual ingesta, using tap water (19). The intestines were then segmented into sections approximately 10 cm in length, which were rigorously rinsed with a saline solution (20). Subsequently, layers including the tunica serosa, tunica muscularis, and mucosa were mechanically separated to isolate the SIS layer. This layer was further cleansed through multiple washes with a saline solution.

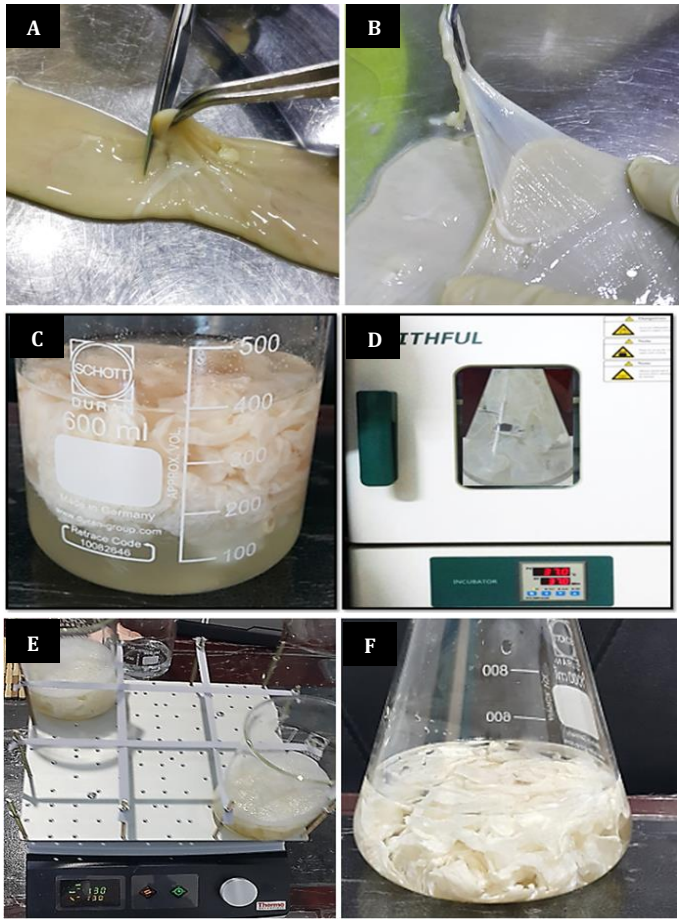

Figure 1. The preparation and decellularization of Small Intestine Submucosa (SIS). **(A)** Cutting the small intestine in length of approximately 10 cm and washed with a saline solution.**(B)** Mechanical removal of the tunica serosa, tunica muscularis and mucosa. **(C)** SIS submerge in methanol and chloroform (1:1, V/V) for 12 h. **(D)** SIS was incubated in the 0.05% trypsin 0.05% ethylenediamine tetra acetic acid at 37 C for 12 h. **(E)** SIS treated with 0.5% sodium dodecylsulphate (SDS) in 0.9% sodium chloride by continuously shaking on an orbital shaker for 4 hr. **(F)** Soaking SIS into 0.1% peroxyacetic acid and 20% ethanol for 30 min

The isolated submucosal membranes were immersed in a solution composed of 100% methanol (Haymankimia®) and 99.8% chloroform (SDFCL, India) in a 1:1 v/v ratio for 12 h, followed by extensive washing with deionized water to remove residual organic solvents. The membranes were incubated in a 0.05% trypsin (HIMEDIA®, India) and 0.05% ethylenediaminetetraacetic acid (EDTA, SDFCL, India) solution at 37 °C for 12 h. Post trypsin treatment, the membranes were continuously washed with a saline solution to completely remove the enzyme. A third treatment involved exposing the membranes to 0.5% sodium dodecyl sulfate (SDS) (Alpha Chemika, India)

dissolved in 0.9% sodium chloride, conducted under continuous agitation on an orbital shaker for 4 h. The membranes were then thoroughly rinsed with a saline solution to eliminate the detergent. Finally, the decellularized membranes were treated with a solution of 0.1% peroxyacetic acid and 20% ethanol (100% Chem-Lab, Belgium) for 30 min. After this treatment, the membranes were rinsed with saline solution to ensure the removal of all chemical residues.

Upon completion of the decellularization process, sections of the SIS samples were cut and stained with hematoxylin and eosin (H&E). These stained sections were then evaluated histologically to determine the extent of cellular removal. All samples were subsequently freeze-dried under -70 °C overnight in a lyophilizer and sealed in airtight packages for preservation (21).

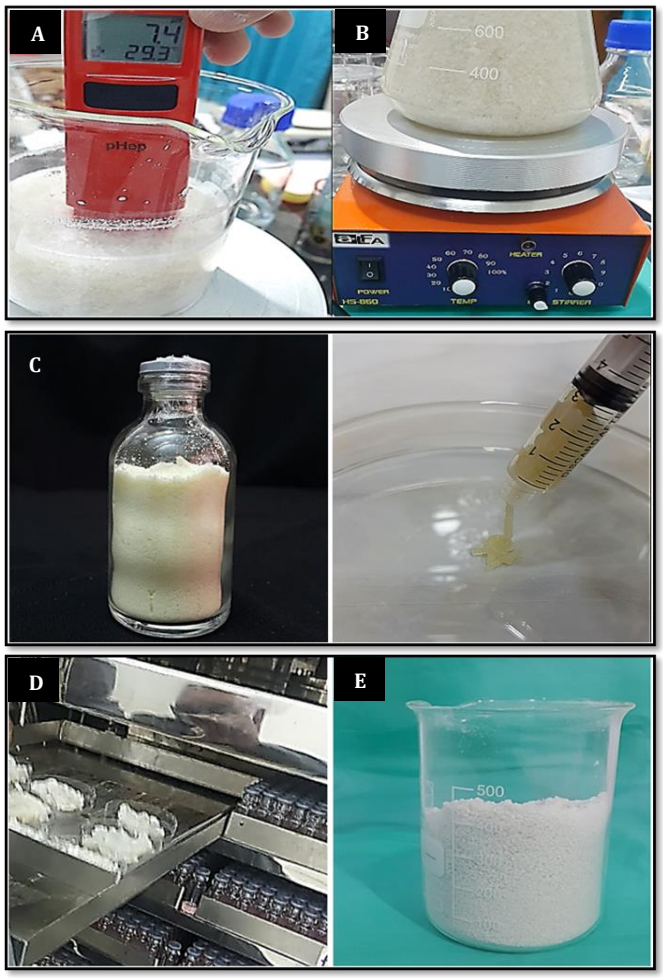

Figure 2. The preparation of Small Intestine Submucosa (SIS) hydrogel; **(A)**. All SIS pieces frozen-dried under -70 °C overnight with a lyophilizer. **(B)** Pulverization of lyophilized SIS. **(C)** Suspending of Pulverized SIS in 1 mg/mL pepsin in 0.01 M HCl for 72 h., stirred (60 rpm) constantly for 48 h. at room temperature, adjusted to pH 7.4. **(D)** Lyophilized and powdered of digested SIS, sealed into airtight packages. **(E)** SIS-hydrogel after dissolving SIS powder in PBS and incubated overnight at 37 °C.

Preparation of SIS Hydrogel

The SIS hydrogel was prepared according to Zhao et al., 2020 (22) with modification as follow; The SIS pieces were pulverized, suspended in HCl (Honeywell, Fluka®) solution with pepsin (HIMEDIA®, India) (Pepsin 1 mg/mL in 0.01 M HCl for 72 h), stirred (60 rpm) constantly for 48 h. optimized for pH 7.4 at room temperature, lyophilized (-70 °C) and powdered using electrical mill after incubation liquid nitrogen tank for 3 h to obtain an SIS powder, packed in airtight containers, then gamma-irradiated (25 KGY) (60Co gamma cell 220 Excel, Canada) to sterilize them and stored at -20 °C until use. The SIS powder dissolved in phosphate-buffered saline PBS at 50% w/v and molded into a hydrogel overnight at 37 °C (Figure. 2). Based on the excellent fluidity of hydrogel, it can be applied with a syringe to a specified site.

Characterization of the SIS Hydrogel

Fourier transform infrared spectroscopy (FTIR)

The chemical structure of hydrogel was identified using the FTIR method. This technique is based on excitement and absorption of infrared light at frequencies that are typically correlated to the types of chemical bonds. The hydrogel samples were introduced in the FTIR spectrometer (8400S, Shimadzu, Japan) with a spectral range of 4000-400 cm^{-1}, attenuated total reflection mode, and a resolution of 4 cm to investigate the structural arrangement in hydrogel was done (23).

Swelling ratio (Sr) measurement

The equilibrium degree of swelling (swelling ratio) of the hydrogels was measured using the method previously mentioned by Qin et al. (24). The known weight of dried hydrogel (W-Dry) was submerged in phosphate-buffered saline (PBS) for 12 h at 37 °C. After swelling, the distilled water was aspirated and blotted the hydrogel with filter paper to remove the surface water and weighed again (W-Wet). The swelling ratio was calculated as $SR=(m_2 - m_1)/m_1$, where m_2 is the weight of the swollen hydrogel, and m_1 is the weight of the dried hydrogel.

Scanning electron microscopy (SEM)

The topography and surface morphology of the hydrogels were examined using a Zeiss Supra 55vp SEM, Germany. The hydrogel samples were first freeze-dried at -70 °C for 6 hours. After freeze-drying, cross sections were carefully obtained from the dried samples using a sharp, cold blade. These cross sections were then examined under the Zeiss Supra 55vp SEM (25).

Antimicrobial Activity of Hydrogels

Methicillin resistant *Staphylococcus aureus* (MRSA) was previously isolated from the milk of clinical mastitis ewes and then bacteriologically identified via culturing, microscopically, biochemically, and an antimicrobial susceptibility test. The MRSA was cultured on Muller-Hinton agar (HiMedia®, India) from the broth. After finishing the culturing, 1 well was made in the agar in a way that does not touch the dish bottom surface, for ensuring of

a proper distribution of the. SIS hydrogel which was put into the well. The dish was sealed and left in an incubator at 37 °C for 24 h, to be read in the next day through the measurement of the diameter of the inhibition zone around well (mm) using a caliper to evaluate the antibacterial activity (26). These examinations were carried out using level 3 biosafety cabinet in the laboratory of Zoonotic Diseases Unite, College of Veterinary Medicine, University of Baghdad.

RESULTS AND DISCUSSION

Histology of SIS

The histological section of bovine small SIS before decellularization, shows collagen stroma infiltration with various types of cells including fibroblasts, fibrocytes, mast cells and monocytes (Figure 3 a). The decellularized SIS membrane appeared as dense collagen stroma (Figure 3 b).

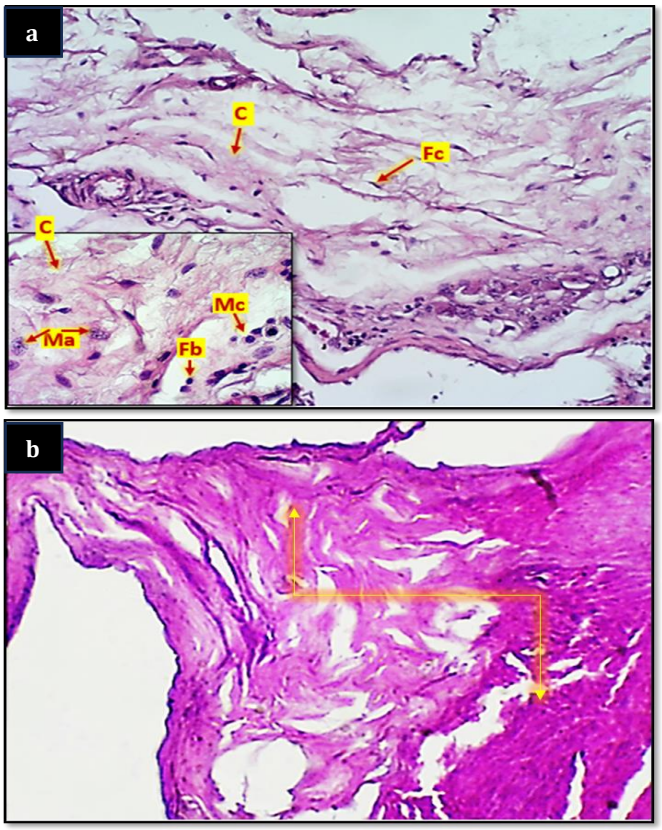

Figure 3. (a) Microscopical section of bovine small intestinal submucosa before decellularization showing collagen stroma **(C)** infiltrate with various types of cells including fibroblasts **(Fb)**, fibrocytes **(Fc)**, mast cells **(Ma)**, momocytes **(Mc)**. (H& E stain10 and 40X. **(b).** Microscopical section of decellularized bovine small intestinal submucosa shows collagen fibers **(arrow)** without cells. H&E stain, 40×

Characterization of the SIS Hydrogel

FTIR

FTIR was used to identify the chemical structure of the SIS hydrogel (Figure 4). The FTIR spectrum of SIS hydrogel showed several absorption peaks that mainly return for the amide groups vibrations, the major functional groups of collagens have distinct peaks that have been found. The spectrum contained three main peaks amide I (1639 cm^{-1}) for C=O vibration appeared overlapping with amide II (1571 cm^{-1}) which were primarily credited N-H bending, and amide III (1338 cm^{-1}) bands for C–N stretching. These characteristic peaks associated with the main functional groups in collagens were also reported by (27). The N-H stretching vibration was observed at (3261 cm^{-1}). Many other peaks were also observed, such as a broad signal at (3440 cm^{-1}) was observed corresponding to the stretching of O-H bonds may be related to side chain of hydroxyproline, in agreement with study by (28) which was applying the X-ray photoelectron spectrometer (XPS) to confirm the FTIR data. Also, CH_2 vibration of the glycine backbone and that of the proline side chain at 1228 -1242 cm^{-1}, same peaks were detected by (29) after analysis of commercial components collagen type I. Furthermore, a spectral band between 2935-2979 cm^{-1} representing the CH_2-asymmetric vibration mode and that of the CH_3-asymmetric vibration mode has also been observed by (30) in skin collagen as amide B.

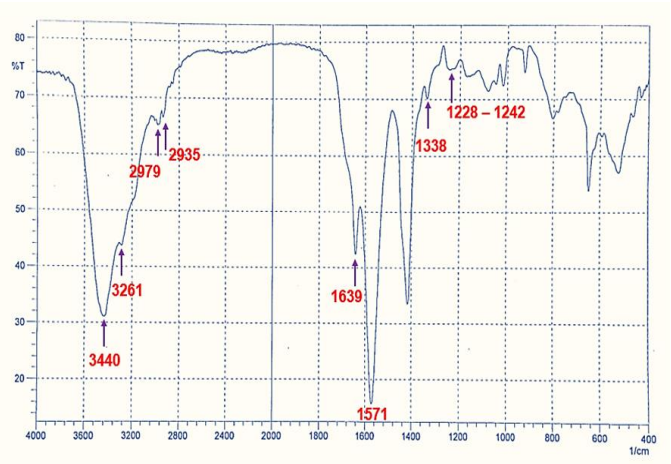

Figure 4. Fourier transform infrared spectrum of SIS hydrogel shows the three main peaks of 1639 cm^{-1}, 1571 cm^{-1}, and 1338 cm^{-1} related to amide I, II and III, respectively, and many other peaks were also observed, such as broad signal at 3440 cm^{-1}) related to side chain of hydroxyproline

Sr measurement

The equilibrium swelling capacities of SIS hydrogel in present study was 437% after immersion in PBS with pH of 7.4 for 12 h (Figure 5). This result indicates that the SIS hydrogel is hydrophilic and has a good ability to absorb water and fluid. The hydrophilicity of SIS hydrogel may be related to its chemical bonds, particularly the carboxyl-amide group. This argument was verified by (31), who indicated that the presence of a carboxyl-amide group in hydrogel triggers the polymer network to expand so that it can imbibe the water easily.

The swelling feature is important for hydrogel which is used in medical applications because it absorbs tissue exudates and offers a moist environment for the open wound. Support cell attachment and increase the speed of

cell migration. Moreover, functionalization with loaded therapeutic agents and sustained release mechanism (32-36). The hydrogel swelling ratio can also determine the hydrogels cross-linking density (CLD) since the swelling ratio increases at higher cross-linking density of gel (37). The CLD represents to the amount of interconnected polymer chains per unit volume of hydrogel (polymer network) that is responsible for the formation and maintenance of the hydrogel structure (38). Furthermore, the improvement in crosslinking density reflects that the hydrogel is composed of a high number of functional groups (39). In addition to the fact that crosslinking aids in retaining a significant amount of water, it also renders the hydrogel insoluble in water or biological fluids (40).

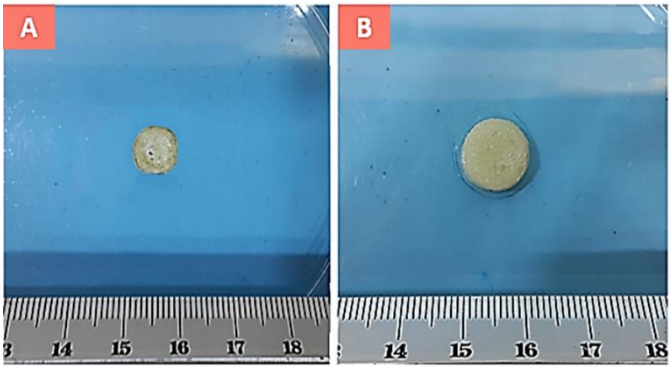

Figure 5. Shows swelling ratio of SIS hydrogel. **(A)** The full dried SIS hydrogel, and **(B)** Swollen SIS hydrogel sample after immersion in PBS for 12 hours at 37Co

Wang et al. (41) recorded a higher swelling ratio of SIS hydrogel compering to collagen type I hydrogel and showed that the increasing in concentration of SIS hydrogel leads to increase in swelling ratio due to increase of gel cross-linking density. The keratin hydrogel swelling properties were studied by Ramos et al. (42), who observed a high swelling ratio up to 650 % at pH 8 remarkably higher than that at pH 6 which was around 100% and concluded that the minimum swelling is noticeable at low pH, a significant rise of swelling was observed above pH 6 and reached the maximum above pH 8. That reveals there is a relationship between environmental pH and swelling ratio. Zhao et al. (36) confirmed the sensitivity of SIS hydrogel to pH, and also observed that a higher SIS content results in higher swelling ratio and attributed that to the SIS is more hydrophilic due to its highly water contact angle. All above these previous studies which discussed the swelling property with different type and concentration of hydrogels supported the result of swelling ratio calculation of current study and confirm the formation of a moist microenvironment with crosslinking density and appropriate porosity.

SEM

Scanning the lyophilized hydrogel by electron microscopy, showed a relatively smooth external surface with many cracks without any pores while the cross section exhibited highly porous and interconnected architecture like honeycomb the results are shown in (Figure 6).

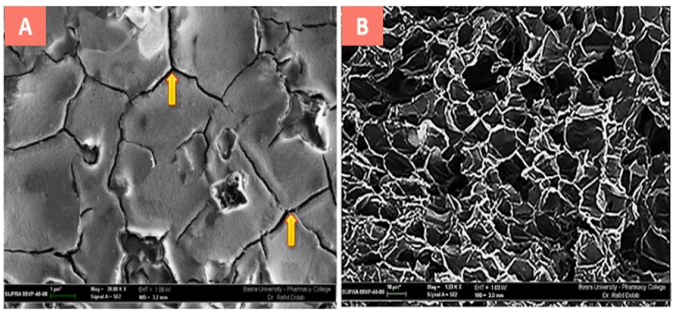

Figure 6. SEM photographs of lyophilized SIS hydrogel, **(A)** External surface shows smooth external surface with many cracks (arrows) (magnification 20.00 KX). **(B)** Cross section of lyophilized hydrogel shows pores and interconnected architecture like honeycomb (magnification 1.53 KX)

This result is relatively consistent with result of (43) who researched how hydrogels changed morphologically in various buffered pH solutions and examined SEM images of freeze-dried gel swelled in pH 7.4 buffer solution, which exhibited regular porous honeycomb-like architectures. SEM Study of the 2% SIS hydrogel by (44) displayed a highly microporous structure with an average pore size of 143 µm and discovered that greater pore size indicated better cell adhesion and proliferation. The same study also discovered that the cell count in 2% SIS hydrogel was higher than that in 1% SIS hydrogel. Moreover, the microstructure of the 15% w/v lyophilized small intestine submucosa hydrogel prepared by (45) possessed sufficiently high porosity in SEM analysis which was facilitate survival of the cells. The SEM findings in the present study indicate that prepared SIS hydrogel is an adequate bio-scaffold, depending on its morphology and porous topology, which can support cell adhesion, migration, and proliferation.

Antibacterial Activity of SIS Hydrogel

In current study, the antimicrobial efficiency of the SIS hydrogel was evaluated against MERSA, by application of agar diffusion test and assessed the zone of inhibition. The SIS hydrogel in present study displayed a zone of inhibition of 16.11 mm (Figure 7).

Figure 7. Agar diffusion test of SIS hydrogel shows 16.11 mm zoon of inhibition

These results refer to suppression of the SIS hydrogel to bacterial growing. Numerous studies investigated intact ECM and ECM fragments to test their ability to control infection and to determine the mechanisms by which biological scaffolds resist the bacterial infections. Sarikaya et al. (46) showed that ECMs derived from SIS (small intestinal submucosa) extract of porcine was found to demonstrate antimicrobial activity against E. coli and S. aureus. A commercial graft of SIS was s applied by Shell et al. (47) in closure of the abdominal defects of pigs, the SIS scaffold shown the ability to resist of *S. aureus* colonization. The scaffold elements made from small intestinal matrix have shown to have similar function, when (48) evaluated it in stifle joint defect in a dog model after induced infection with *S. aureus* without any antibiotics administration, this study shown well integration of SIS-scaffold to host tissue and the microbiological culture of joint fluid was negative. Likewise, the Sarikaya et al. (46) reported that ECM extracts of acellular SIS matrices has antibacterial activity against S. aureus and *E. coli*. A study by Jernigan et al. (49) showed the superiority of SIS as angioplasty patch a compered to polytetrafluoroethylene (PTFE) with presence of massive gastrointestinal contamination and explain this ability to presence of a peptide in fresh SIS specimens that has antimicrobial properties (7), as well as Medberry et al. (50) showed the greater resistance of biologic scaffolds to infection when compared with the synthetic surgical mesh repair in a rat model of abdominal body wall repair.

Usually, the small intestine submucosa is often exposed to a variety of bacteria, and it continuously produces antimicrobial peptides to regulate the development of the macrobiotic (51). The degradation products of ECM scaffold develop bioactive fragment and exert antimicrobial effect (52). The bioactive peptides called cryptic peptides or matricrypteins developed through partial proteolysis of extracellular matrix macromolecules (53) such as, glycoproteins elastin, and collagen these matricrypteins have various effects such as chemotaxis cells adhesion, angiogenic, antimicrobial and antioxidant functions (54, 55, 56). Study by Abdillahi et al. (57) shown that alpha 3 subunit of type VI collagen causes distraction of bacterial extracellular membrane of E. coli and S. aureus. Andersson et al. (52) explained that there are some peptides derived from vitronectin, fibronectin and laminin exhibit antimicrobial activity against Gram-negative and Gram-positive bacteria.

Furthermore, the scaffolds prepared from decellularized ECM growth factors such as platelet-derived growth factor (PDGF), hepatocyte growth factor (HGC) and fibroblast growth factors (FGF) display bactericidal activity against Gram positive and Gram-negative bacteria (51, 58, 59).

In conclusion, the bovine SIS can be easily separated from other layers. The time required for decellularization of the SIS was approximately 30 hours, after successive treatment with chemicals. The SIS pieces were pulverized, lyophilized (-70 °C) and powdered. PBS was used to dissolve the obtained SIS powder at 50% w/v (50 mg/mL) and formed into a gel for 12 hours at 37 °C. the hydrogel in present study chemically composed of amide type I, II and III, proline, hydroxyproline and glycine. In addition the hydrogel possessed high swelling ratio, highly porous with interconnected architecture as well as antibacterial activity. These findings of hydrogel are expected to be ideal bio-scaffold for accelerated healing of damaged tissues and to be used in regenerative medicine.

ACKNOWLEDGEMENTS

N/A

CONFLICT OF INTEREST

The authors declare no conflict of interest.

REFERENCES

1. Denost Q, Adam J, Pontallier A, Montembault A, Bareille R, Siadous R, et al. Colorectal tissue engineering: A comparative study between porcine small intestinal submucosa (SIS) and chitosan hydrogel patches. Surgery. 2015;158(6):1714–1723.
2. Al-Falahi NH, Abood D, Dauood MS. Comparative evaluation of bovine pericardial membrane and amniotic membrane in wounds skin healing in rabbits. Iraqi J Vet Med. 2017;41(2):137–145.
3. Al-Bayati AHF, Al-Tememe HA, Al-Mudallal NH. Role of acellular bovine urinary bladder submucosa on skin wound healing in Iraqi goats. Iraqi J Vet Med. 2016;40(1):53–60.
4. Gautam S, Ambwani S. Tissue Engineering: New Paradigm of Biomedicine. Biosci Biotech Res Asia. 2019;16(3):521–532.
5. Al-ebadi AKM, Al-Bayati AHF. Effect of acellular bovine pericardium and urinary bladder submucosa matrixes in reconstruction of ventro-lateral hernias in bucks; molecular evaluation. Iraqi J Vet Med. 2019;43(1):67–74.
6. Ekder ES, Mahdi AK. Augmentation cystoplasty using autograft of thigh fascia lata: experimental study in canine model. Annal Rom Soc Cell Biol. 2021;25(3):3029–3039.
7. Al-Falahi NH. Comparative study for using of sub mucosa of small intestine in healing of clean and infected avulsion wounds. Iraqi J Vet Med. 2009;33(1):89–97.
8. Capella-Monsonís H, Tilbury MA, Wall JG, Zeugolis DI. Porcine mesothelium matrix as a biomaterial for wound healing applications. Materials Today Bio. 2020;7:100057.
9. Saldin LT, Cramer MC, Velankar SS, White LJ, Badylak SF. Extracellular matrix hydrogels from decellularized tissues: Structure and function. Acta Biomater. 2017;49:1–15.
10. Mahmood MM, Mahdi AK. Experimental study of the effect of Plantago major leaves extract on contaminated excisional wound healing in rabbits. Iraqi J Vet Sci. 2022;36(1):31–9.
11. Mohammed MS, Salih SI. Histopathological study of using fetal caprine acellular dermal matrix alone and in combination with Non-thermal plasma in healing of full-thickness acute skin wounds in bucks. Int J Health Sci. 2022;6(S3):8784–806.
12. Zambon JP, Atala A, Yoo JJ. Methods to generate tissue-derived constructs for regenerative medicine applications. Methods. 2020;171:3–10.
13. Singh H, Purohit SD, Bhaskar R, Yadav I, Gupta MK, Mishra NC. Development of decellularization protocol for caprine small intestine submucosa as a biomaterial. Biomaterials and Biosystems. 2022;5 100035:2666–5344.
14. AL-Falahi NH, Salih SI. A comparative histopathological study of repaired tendons wrapped with two biological matrices in bucks. Adv Anim Vet Sci. 2016;4(3):145–52.

15. Rashtbar M, Hadjati J, Ai J, Jahanzad I, Azami M, Shirian S, et al. Characterization of decellularized ovine small intestine submucosal layer as extracellular matrix-based scaffold for tissue engineering. J Biomed Mater Res B Appl Biomater. 2018;106(3):933–44.
16. Majee SB. Emerging Concepts in Analysis and Applications of Hydrogels. London: IntechOpen; 2016. 266 p.
17. González-Díaz EC, Varghese S. Hydrogels as Extracellular Matrix Analogs. Gels. 2016;2(3):20.
18. Zhang W, Du A, Liu S, Lv M, Chen S. Research progress in decellularized extracellular matrix-derived hydrogels. Reg Ther. 2021;18:88–96.
19. White LJ, Keane TJ, Smoulders A, Zhang L, Castleton A, Badylak SF. The effects of terminal sterilization upon the biological activity and stiffness of extracellular matrix hydrogels. Front Bioeng Biotechnol. 2016; Conference Abstract: 10th World Biomaterials Congress.
20. Claudio-Rizo JA, Mendoza-Novelo B, Delgado J, Castellano LE, Mata-Mata JL. A new method for the preparation of biomedical hydrogels comprised of extracellular matrix and oligourethanes. Biomed Mater. 2016;11(3):035016.
21. Luo JC, Chen W, Chen X, Qin T, Huang YC, Xie HQ, et al. A multi-step method for preparation of porcine small intestinal submucosa (SIS). Biomaterials. 2011;32(3):706–13.
22. Zhao P, Li X, Fang Q, Wang F, Ao Q, Wang X, et al. Surface modification of small intestine submucosa in tissue engineering. Regen Biomater. 2020;7(4):339–48.
23. Perez-Puyana V, Jimenez-Rosado M, Romero A, Guerrero A. Fabrication and characterization of hydrogels based on gelatinised collagen with potential application in tissue engineering. Polymers. 2020;12(5):1146.
24. Qin H, Wang J, Wang T, Gao X, Wan Q, Pei X. Preparation and characterization of chitosan/β-glycerophosphate thermal-sensitive hydrogel reinforced by graphene oxide. Front Chem. 2018;6:565.
25. Azeera M, Vaidevi S, Ruckmani K. Characterization techniques of hydrogel and its applications. In: Mondal M, editor. Cellulose-based superabsorbent hydrogels. Polymers and polymeric composites: a reference series. Cham: Springer; 2019.
26. Imade EE, Omonigho SE, Babalola OO, Enagbonma BJ. Lactic acid bacterial bacteriocins and their bioactive properties against food-associated antibiotic-resistant bacteria. Ann Microbiol. 2021;71(1):44.
27. Duan L, Yuan Q, Xiang H, Yang X, Liu L, Li J. Fabrication and characterization of a novel collagen-catechol hydrogel. J Biomater Appl. 2018;32(7):862–70.
28. Scheglov A, Helmke A, Loewenthal L, Ohms G, Vioel W. XPS and ATRFTIR study on chemical modifications of cold atmospheric plasma (CAP) operated in air on the amino acids L-proline and trans-4-hydroxy-Lproline. Plasma Process Polym. 2018;15:e1800078.
29. Sanden KW, Kohler A, Afseth NK, Böcker U, Rønning SB, Liland KH, et al. The use of Fourier-transform infrared spectroscopy to characterize connective tissue components in skeletal muscle of Atlantic cod (Gadus morhua L.). J Biophotonics. 2019;12(9):e201800436.
30. Riaz T, Zeeshan R, Zarif F, Ilyas K, Muhammad N, Safi SZ, et al. FTIR analysis of natural and synthetic collagen. Appl Spectrosc Rev. 2018;53(9):703–746.
31. Hebeish A, Hashem M, Abd El-Hady MM, Sharaf S. Development of CMC hydrogels loaded with silver nano-particles for medical applications. Carbohydr Polym. 2013;92(1):407–13.
32. Schunck M, Neumann C, Proksch E. Artificial barrier repair in wounds by semi-occlusive foils reduced wound contraction and enhanced cell migration and reepithelization in mouse skin. J Invest Dermatol. 2005;125(5):1063–71.
33. Caccavo D, Cascone S, Lamberti G, Barba AA, Larsson A. Swellable hydrogel-based systems for controlled drug delivery. Smart Drug Deliv Syst. 2016;237–303.
34. Onaciu A, Munteanu RA, Moldovan AI, Moldovan CS, Berindan-Neagoe I. Hydrogels based drug delivery synthesis, characterization and administration. Pharmaceutics. 2019;11(9):432.
35. Su C, Gong JS, Ye JP, He JM, Li RY, Jiang M, et al. Enzymatic extraction of bioactive and self-assembling wool keratin for biomedical applications. Macromol Biosci. 2020;20(9):2000073.
36. Zhao LM, Gong M, Wang R, Yuan QJ, Zhang Y, Pi JK, et al. Accelerating ESD-induced gastric ulcer healing using a pH-responsive polyurethane/small intestinal submucosa hydrogel delivered by endoscopic catheter. Regen Biomater. 2021;8(1):rbaa056.
37. Raghuwanshi VS, Garnier G. Characterisation of hydrogels: Linking the nano to the microscale. Adv Colloid Interface Sci. 2019;274:102044. doi: 10.1016/j.cis.2019.102044
38. Hoti G, Caldera F, Cecone C, Rubin Pedrazzo A, Anceschi A, Appleton SL, et al. Effect of the cross-linking density on the swelling and rheological behavior of ester-bridged β-cyclodextrin nanosponges. Materials. 2021;14(3):478.
39. Almawash S, Osman SK, Mustafa G, El Hamd MA. Current and future prospective of injectable hydrogels—design challenges and limitations. Pharmaceuticals [Internet]. 2022;15(3):371.
40. Lee JH. Injectable hydrogels delivering therapeutic agents for disease treatment and tissue engineering. Biomater Res. 2018;22(1):1–4.
41. Wang W, Zhang X, Chao NN, Qin TW, Ding W, Zhang Y, et al. Preparation and characterization of pro-angiogenic gel derived from small intestinal submucosa. Acta Biomater. 2016;29:135–48.
42. Ramos MLP, González JA, Fabian L, Pérez CJ, Villanueva ME, Copello GJ. Sustainable and smart keratin hydrogel with pH-sensitive swelling and enhanced mechanical properties. Mater Sci Eng C. 2017;78:619–26.
43. Sun XW, Hai-hong J, Zhan-xin M, Rajaratnam. Hemicellulose-based pH-sensitive and biodegradable hydrogel for controlled drug delivery. Carbohydr Polym. 2013;92(2):1357–66.
44. Liu G, Li Q, Wang W, Jiang J, Liao J, Ge L, et al. Formulation and characterization of a novel, photoinitiated small intestinal sub-mucosal wound-healing hydrogel. Trop J Pharm Res. 2017;16(7):1473–1480.
45. Kim K, Kim MS. An injectable hydrogel derived from small intestine submucosa as a stem cell carrier. J Biomed Mater Res B Appl Biomater. 2016;104(8):1544–1550.
46. Sarikaya A, Record R, Wu CC, Tullius B, Badylak S, Ladisch M. Antimicrobial activity associated with extracellular matrices. Tissue Eng. 2002;8(1):63–71.
47. Shell DH, 4th, Croce MA, Cagiannos C, Jernigan TW, Edwards N, Fabian TC. Comparison of small-intestinal submucosa and expanded polytetrafluoroethylene as a vascular conduit in the presence of gram-positive contamination. Ann Surg. 2005;241(6):995–1004.
48. Badylak SF, Wu CC, Bible M, McPherson E. Host protection against deliberate bacterial contamination of an extracellular matrix bioscaffold versus Dacron mesh in a dog model of orthopedic soft tissue repair. J Biomed Mater Res B Appl Biomater. 2003;67(1):648–654.
49. Jernigan TW, Croce MA, Cagiannos C, Shell DH, Handorf CR, Fabian TC. Small intestinal submucosa for vascular reconstruction in the presence of gastrointestinal contamination. Ann Surg. 2004;239(5):733.
50. Medberry CJ, Tottey S, Jiang H, Johnson SA, Badylak SF. Resistance to infection of five different materials in a rat body wall model. J Surg Res. 2012;173(1):38–44.
51. Jiménez-Gastélum GR, Aguilar-Medina EM, Soto-Sainz E, Ramos-Payán R, Silva-Benítez EL. Antimicrobial properties of extracellular matrix scaffolds for tissue engineering. BioMed Res Int. 2019;2019: 1–11.
52. Andersson E, Rydengård V, Sonesson A, Mörgelin M, Björck L, Schmidtchen A. Antimicrobial activities of heparin-binding peptides. Eur J Biochem. 2004;271(6):1219–1226.
53. Ner J, Kotlinska J, Silberring J. Crypteins-an overlooked piece of peptide systems. Curr Protein Pept Sci. 2015;16(3):203–218.
54. Maquart FX, Pasco S, Ramont L, Hornebeck W, Monboisse JC. An introduction to matrikines: extracellular matrix-derived peptides which regulate cell activity: implication in tumor invasion. Crit Rev Oncol Hematol. 2004;49(3):199–202.

55. Lopresti ST, Brown BN. Host response to naturally derived biomaterials. In: Badylak SF, Gilbert TW, editors. Host response to biomaterials. Academic Press; 2015. p. 53–79.
56. Sivaraman K, Shanthi C. Matrikines for therapeutic and biomedical applications. Life Sci. 2018;214:22–33.
57. Abdillahi SM, Maaß T, Kasetty G, Strömstedt AA, Baumgarten M, Tati R, et al. Collagen VI contains multiple host defense peptides with potent in vivo activity. J Immunol. 2018;201(3):1007–20.
58. Malmsten M, Davoudi M, Walse B, Rydengård V, Pasupuleti M, Mörgelin M, et al. Antimicrobial peptides derived from growth factors. Growth Factors. 2007;25(1):60–70.
59. Gupta SK, Dinda AK, Mishra NC. Antibacterial activity and composition of decellularized goat lung extracellular matrix for its tissue engineering applications. Biol Eng Med. 2017;2(1):1–7.

تحضير وتوصيف الهلام الماي من الطبقة تحت المخاطية للأمعاء الدقيقة

صدام خالد حمادي[١]، نادية حميد رجة الفلاحي[٢]

[١]فرع الجراحة والتوليد، كلية الطب البيطري، جامعة تكريت، تكريت، العراق، [٢]فرع الجراحة والتوليد، كلية الطب البيطري، جامعة بغداد، بغداد العراق

الخلاصة

كان الهدف من الدراسة الحالية هو تحضير وتوصيف هيدروجيل الأمعاء الدقيقة تحت المخاطية كسقالة حيوية. في هذه الدراسة ، تم الحصول على الطبقة تحت المخاطية للأمعاء الدقيقة (SIS) لخمسة عجول، تتراوح أعمارهم بين ٨-١٢ شهرًا ووزنها ٢٥٠-٣٠٠ كجم) من المجزرة مباشرة بعد الذبح، ثم تم نزع الخلايا من هذه الطبقة وتحويلها الى مسحوق. تم تحضير الهلام المائي من الطبقة تحت المخاطية للأمعاء الدقيقة عن طريق إذابة مسحوق تحت المخاطية للامعاء الدقيقة (SIS) منزوع الخلايا في محلول الفوسفات الملحي المنظم (PBS) بتركيز ٥٠ ٪ وزن / حجم (٥٠ مجم / مل) حيث تشكل هذا المزيج الى هلام بعد وضعه في الحاضنة طوال الليل عند ٣٧ درجة مئوية. تم توصيف الهلام المائي بواسطة مطيافية الأشعة تحت الحمراء باستخدام تحويل فورييه (FTIR) ، ونسبة التورم ، والفحص المجهري الإلكتروني (SEM) والنشاط المضاد للميكروبات للهلام المائي. تم تحديد التركيب الكيميائي للهيدروجيل باستخدام طريقة FTIR. احتوى الطيف الاشعة تحت الحمراء (FTIR) على ثلاث قمم رئيسية (١٦٣٩ سم $^{-١}$) (١٥٧١ سم $^{-١}$) و (١٣٣٨ سم $^{-١}$) التي تعود الى الأميد الأول والثاني والثالث على التوالي ، ولوحظ أيضًا العديد من القمم الأخرى ، مثل الإشارة العريضة عند (٣٤٤٠ سم -١) التي تتعلق بالسلسلة الجانبية للهيدروكسي برولين. اما قدرة التورم لهلام تحت مخاطية الامعاء الدقيقة في الدراسة الحالية كانت ٤٣٧٪ بعد الغمر في محلول الفوسفات الملحي المنظم (PBS) بدرجة حموضة ٧،٤ لمدة ١٢ ساعة. أظهر مسح المجهر الإلكتروني (SEM) للهلام المائي المجفف بالتجميد ، بنية مسامية مترابطة للغاية تشبه قرص العسل. علاوة على ذلك ، تم اختبار فعالية الهلام المضادة للبكتيريا ضد بكتيريا المكورات العنقودية الذهبية باستخدام اختبار انتشار الاجار حيث اظهر منطقة تثبيط تبلغ ١١،١٦ ملم. الخصائص الكيميائية والبنية التركيبية والشكلية (المورفولوجية)فضلاً عن التأثير المضاد للبكتيريا التي أظهرها الهلام المائي المحضر في الدراسة الحالية من الممكن ان ترشحه كسقالة حيوية تعمل كبديل حيوي يستخدم لتحفيز عملية التجديد التي تعيد الأنسجة الى وظيفتها.

الكلمات المفاحية: تحت مخاطية الأمعاء الدقيقة (SIS) ، نزع الخلايا ، الهلام المائي ، مصفوفة خارج الخلية